View metadata, citation and similar papers at core.ac.uk

brought to you by CORE

provided by Carolina Digital Repository

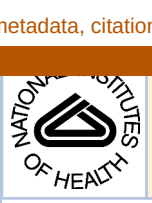

NIH Public Access

Author Manuscript

Hepatology. Author manuscript; available in PMC 2007 January 9.

Published in final edited form as:

Hepatology. 2007 January ; 45(1): 205–212.

Arsenic Stimulates Sinusoidal Endothelial Cell Capillarization and Vessel Remodeling in Mouse Liver

Adam C. Straub[1], **Donna B. Stolz**[2], **Mark A. Ross**[2], **Araceli Hernández-Zavala**[3], **Nicole V. Soucy**[4], **Linda R. Klei**[1], and **Aaron Barchowsky**[1]

1 *From the Department of Occupational and Environmental Health, University of Pittsburgh Graduate School of Public Health, Pittsburgh, PA;*

2 *Department of Cell Biology, University of Pittsburgh, Pittsburgh, PA;*

3 *Center for Environmental and Molecular Biology of the Lung, University of North Carolina, Chapel Hill, NC; and*

4 *Dartmouth Medical School, Hanover, NH.*

Abstract

—Trivalent arsenic [As(III)] is a well-known environmental toxicant that causes a wide range of organ-specific diseases and cancers. In the human liver, As(III) promotes vascular remodeling, portal fibrosis, and hypertension, but the pathogenesis of these As(III)-induced vascular changes is unknown. To investigate the hypothesis that As(III) targets the hepatic endothelium to initiate pathogenic change, mice were exposed to 0 or 250 parts per billion (ppb) of As(III) in their drinking water for 5 weeks. Arsenic(III) exposure did not affect the overall health of the animals, the general structure of the liver, or hepatocyte morphology. There was no change in the total tissue arsenic levels, indicating that arsenic does not accumulate in the liver at this level of exposure. However, there was significant vascular remodeling with increased sinusoidal endothelial cell (SEC) capillarization, vascularization of the peribiliary vascular plexus (PBVP), and constriction of hepatic arterioles in As(III)-exposed mice. In addition to ultrastructural demonstration of SEC defenestration and capillarization, quantitative immunofluorescence analysis revealed increased sinusoidal PECAM-1 and laminin-1 protein expression, suggesting gain of adherens junctions and a basement membrane. Conversion of SECs to a capillarized, dedifferentiated endothelium was confirmed at the cellular level with demonstration of increased caveolin-1 expression and SEC caveolae, as well as increased membrane-bound Rac1-GTPase.

Conclusion— These data demonstrate that exposure to As(III) causes functional changes in SEC signaling for sinusoidal capillarization that may be initial events in pathogenic changes in the liver.

Abbreviations

ECM, extracellular matrix; NO, nitric oxide; PBVP, peribiliary vascular plexus; PECAM-1, platelet endothelial cell adhesion molecule (CD31); SEC, sinusoidal endothelial cell; SEM, scanning electron microscopy; TEM, transmission electron microscopy; VEGF, vascular endothelial cell adhesion molecule

Address reprint requests to: Aaron Barchowsky, Ph.D., University of Pittsburgh Graduate School of Public Health, Department of Occupational and Environmental Health, Bridgeside Point, 100 Technology Drive, Rm 332, Pittsburgh, PA 15219. E-mail: aab20@pitt.edu; fax: 412-624-9361..

Potential conflict of interest: Dr. Stoltz and Dr. Barchowsky received grants from NIH. Dr. Straub received grants from University of Pittsburgh. Dr. Savay received grants from Dartmouth Medical School.

Supported by National Institute of Environmental Health Sciences grant ES07373 (to A.B.), National Cancer Institute grant CA76541 (to D.S.), and Environmental Protection Agency STAR Fellowship FP-91654201 (to A.S.).

NIH-PA Author Manuscript

NIH-PA Author Manuscript

NIH-PA Author Manuscript

NIH-PA Author Manuscript

NIH-PA Author Manuscript

NIH-PA Author Manuscript

The vascular effects of arsenic are a global public health concern that contribute to disease in tens of millions of people worldwide.[1] Whereas the role of environmental contaminants in the etiology of vascular diseases and in the vascular contributions to organ dysfunction remains poorly defined, epidemiological studies have associated As(III) exposures to increased risk of cardiovascular diseases[1] and vascular contributions to liver disease.[2] Liver effects associated with arsenic in drinking water include noncirrhotic portal fibrosis and, to a lesser extent, portal hypertension.[2,3] These pathologic conditions involve increased vascular channels in the portal regions of the liver. Higher levels of chronic As(III) consumption increase urinary levels of porphyrins, a biomarker for liver injury, which are more pronounced in people under 20 years of age.[4] In addition, cardiac and liver disorders are the major side effects of therapeutic As(III) regimes that treat leukemias.[5] Despite epidemiological evidence that the liver vasculature is a pathogenic target of chronic As(III) ingestion,[2] the direct effects of As(III) on liver vascular cells are unknown.

In other vascular beds and isolated cell cultures, As(III) affects both endothelial and smooth muscle cell physiology. Arsenic(III) stimulates angiogenic processes in cultured endothelial cells and neovascularization in intact mouse and avian models.[6–9] These angiogenic effects promote tumorigenesis in mice, as well as vascular remodeling.[10,11] Stimulation of endothelial cell proliferation occurs at concentrations of As(III) that are not cytotoxic, whereas higher concentrations are cytotoxic and inhibit angiogenesis in tumors.[10,11] Arsenic(III) stimulates cultured smooth muscle cells to proliferate and express vascular endothelial cell growth factor (VEGF), a primary mediator of angiogenesis.[12] Although these effects of As (III) on cells from systemic blood vessels are well recognized, there is little data on the effects of As(III) exposures on liver vascular remodeling or specifically on the fenestrated sinusoidal endothelium.

The liver sinusoidal endothelial cells (SECs) are highly specialized fenestrated cells that are unique in the extensive heterogeneity of vascular endothelium.[13] Early in development, these cells differentiate to lose markers of a continuous endothelium, such as junctional expression of platelet endothelial cell adhesion molecule-1 (PECAM-1/CD31) and a basement membrane containing the matrix protein laminin-1.[14] In the differentiation process, the SECs become fenestrated to allow sieving of circulating nutrients, lipids, and lipoproteins for normal liver metabolism.[13] The SEC angiogenic process is different from angiogenesis in endothelial cells of systemic vessels, because there is no increase in sinusoidal vessel number or density. Instead, SEC angiogenesis is a dedifferentiation and maturation process called capillarization with diagnostic hallmarks of SEC defenestration and renewed surface expression of PECAM-1 and laminin-1 proteins.[13,15–18] SEC defenestration and formation of tight intercellular junctions limits transendothelial cell transport.[13,16,19,20] Capillarization precedes vascular remodeling of other liver vessels, such as hepatic arterioles and PBVP, causing blood flow shunting, vascular channel formation, and eventually liver fibrosis.[15,16,21] Liver angiogenesis in general is recognized as an important pathogenic process not only in portal fibrosis, but also in portal hypertension and progression of HCCs.[18,22–25] Finally, animal models have been used to demonstrate that liver capillarization affects the systemic vasculature by decreasing liver metabolism of lipids, lipoproteins, and glucose to promote atherogenesis in response to environmental stresses and aging.[13,26,27]

In mouse tumors or surrogate *in vivo* neovascularization assays, low to moderate levels of As (III) (5–250 ppb) in drinking water are angiogenic.[7,28] However, As(III) effects on the liver endothelium or pathogenic angiogenic processes in the liver are unknown. The aim of this study was to investigate whether a chronic, human-relevant, environmental exposure to As(III) causes SEC dedifferentiation and dysfunctional capillarization in intact mice. The data indicate that prolonged As(III) exposure causes SEC maturation and sustained functional changes in SEC cell signaling.

NIH-PA Author Manuscript

NIH-PA Author Manuscript

NIH-PA Author Manuscript

Materials and Methods

Mouse Exposure

Animal exposures were performed in agreement with institutional guidelines for animal safety and welfare at Dartmouth College and the University of Pittsburgh. C57BL/6N male mice, ages 6–8 weeks weighing approximately 20 g were obtained from Taconic Farms (Hudson, NY) or the National Cancer Institute. Standard mouse chow and drinking water solutions were fed ad libitum for 5 weeks to mice housed in boxes of 3. Fresh drinking water solutions containing 250 ppb sodium arsenite (Fisher Scientific, Pittsburgh, PA) were prepared triweekly using commercially bottled drinking water (Giant Eagle Spring Water, Pittsburgh, PA).

Measurement of Tissue Total Arsenic Levels

Total liver arsenic was measured by hydride generation with atomic fluorescence detection following tissue digestion in phosphoric acid, as described.[29] The limit of detection for inorganic arsenic by this analysis was 15 pg.

Scanning and Transmission Electron Microscopy

Tissues were prepared for SEM and TEM as described.[30]

Morphometric Quantitation of Fenestrae

SEM images from 3 control mice or 3 arsenic-exposed mice were captured. Hepatic zones 1 and 3 were identified based on extracellular matrix (ECM) deposition around the large vessels and visualization of bile ducts. Vessels having excess ECM were considered portal veins (zone 1) and large vessels with little or no ECM were considered central veins (zone 3). Once zones were identified, images from representative regions of 5 sinusoids in each zone were taken at approximately 100 μm from the respective large vessel. Porosity (open area of the sinusoid wall) was calculated using MetaMorph software (Universal Imaging Corp., Downingtown, PA). The total area within a representative region of sinusoid was determined in square micrometers. Within this area, the total open area was quantified. Open areas of fenestrae were summed, divided by the total area, and multiplied by 100 to give the percent porosity. The porosities of the 5 sinusoids in each zone were averaged to give a single value (*n*) per mouse.

Immunofluorescence Microscopy

After 5 weeks of exposure, 5 mice per group were killed with CO_2. Livers were excised, snap frozen in liquid nitrogen, and stored at −80°C until sectioning. Cryostat sections (8 μm) on charged glass slides were fixed for 1 minute in cold methanol. Sections were stained as described[30] using antibodies described in Table 1 and coverslipped using Fluoromount G (Southern Biotech, Birmingham, AL). Fluorescent images were captured with an Olympus Fluoview 500 confocal microscope (Malvern, NY) or a Nikon microphot-FXL microscope, fitted with an Olympus CCD digital camera.

Quantitative Immunofluorescence of Sinusoidal Protein Levels

Five random 400× confocal midlobular images of immunofluorescence signals in liver sections were captured using identical exposure times. Using MetaMorph software, images were color separated, changed to monochrome format, and the threshold pixel values were set to equal levels. Pixel number per 400× field was quantified and the average percentage of positively fluorescent pixels per field in the 5 fields was calculated to give a single value per mouse.

NIH-PA Author Manuscript

NIH-PA Author Manuscript

NIH-PA Author Manuscript

Morphometric Analysis of PBVP

Tissue slices were costained for PECAM-1 and α-SMC actin. Hepatic arteries stained positive for both PECAM-1 and α-SMC actin, veins were predominantly PECAM-1 positive with a slight amount of α-SMC actin, and lymphatic vessels stained slightly for PECAM-1 with no α-SMC actin. Epi-fluorescent images of 2 portal tracts per section of normal or As(III)-exposed livers were captured and exported to MetaMorph. Luminal area of hepatic arteries, as well as wall thickness were captured and compared. Vascularization of the PBVP was measured as the number of PECAM-positive or PECAM/α-SMC actin–positive luminal structures per duct wall.

In Situ Isolation of SEC Membrane Proteins with Colloidal Silica

The luminal SEC membranes of control or As(III)-exposed mice livers were isolated by *in situ* membrane density perturbation technique as described.[31] The proteins in the respective membrane fractions were separated by SDS-PAGE and probed by Western analysis with antibodies described in Table 1.

Statistical Analysis

The values for the control and As(III)-exposed mice were analyzed for statistical differences by unpaired *t* test or 2-way ANOVA using Prizm 4.0 software (GraphPad, San Diego, CA).

Results

Arsenic Does Not Accumulate in the Liver

After 5 weeks of exposure, there were no obvious health differences between the control mice and mice that drank water containing 250 ppb arsenic. The total animal weights and liver/body weight ratio did not vary (data not shown) suggesting that food and water intake was equal between the groups and there was no hepatomegalia. There was also no increase in liver tissue levels of total arsenic in the mice fed arsenic-containing water (control = 3.8 ± 1.3 ng/g tissue; arsenic-exposed = 2.9 ± 1.4 ng/g tissue, n = 6). These data confirm earlier reports that arsenic does not accumulate in mouse liver until drinking water levels exceed 1.0 ppm.[32]

Chronic Low Levels of As(III) Exposure Induced Sinusoidal Capillarization

The effects of As(III) exposure on the ultrastructure of the sinusoidal endothelium were examined using both SEM and TEM. The SECs in normal mice contain numerous sieve plates with open fenestrae (Fig. 1). The sinusoids in As(III)-exposed mice were observably defenestrated and the endothelium was continuous, indicating capillarization (Fig. 1). Quantitative morphometric analysis revealed that As(III) caused a 4-fold to 5-fold decrease in porosity (i.e., open space per unit area; Fig. 1, graph) in either zone 1 or zone 3 of the sinusoids. The surface of the As(III)-exposed sinusoids showed an increase in surface projections, some of which were microvilli from the underlying hepatocytes protruding through the SEC fenestrae (Fig. 1). The TEM images in Fig. 2 confirm that decreased sinusoidal porosity in As(III)-exposed mice was paralleled by increased hepatocyte microvilli filling of the space of Disse. Similar microvilli increases were attributed to a compensatory mechanism to recover lost nutrient uptake.[13,33] In contrast, mitochondria and other organellar structures within the hepatocytes retained normal ultrastructure. The magnified images in Fig. 2B demonstrate As (III)-stimulated loss of fenestrations and gain of a rudimentary basement membrane. Caveolae, sparse in the SECs of control mice, were more evident in the capillarized SECs of the As(III)-exposed mice.

NIH-PA Author Manuscript

NIH-PA Author Manuscript

NIH-PA Author Manuscript

As(III) Induces Sinusoidal PECAM-1 and Lami-nin-1 Protein Expression

As discussed above, capillarized SECs express surface PECAM-1 and develop a laminin-1 containing basement membrane.[13,15,34] Quantitative immunofluorescence measurements were used to determine whether the As(III)-induced ultrastructural changes observed in Figs. 1 and 2 accompanied localized increased expression of these proteins. PECAM-1 expression was selectively increased in sinusoids of As(III)-exposed mice, but not in the endothelium of large vessels, such as the portal veins (Fig. 3A,B). The apparent increase in hepatic artery PECAM-1 staining may have been caused by contraction of the vessel lumen (Fig. 4). Midlobular laminin-1 expression also increased (Fig. 3A) and merging the red and green channels in Fig. 3A revealed punctate laminin-1 staining (focal red staining) that is adjacent to the sinusoidal PECAM-1. This may indicate that protein expression in stellate cells, which are a primary source of laminin-1,[16] was also stimulated by As(III). The stellate cells did not appear activated, because there was no increase in midlobular α-SMC staining (data not shown). Quantitative analysis of the immunostained sections demonstrated that As(III) increased expression of both PECAM-1 and laminin-1 relative to controls (Fig. 3C). As reported,[35] the increase in PECAM-1 protein expression at the cell junctions did not correlate with increased PECAM-1 mRNA levels (data not shown).

As(III) Stimulates Vascularization of the PBVP and Hepatic Artery Contraction

The PBVP is often remodeled in alcohol-induced fibrosis and cirrhosis as the hepatic arterial flow increases to compensate for decreased portal blood flow.[18] Arsenic(III) also promoted vascular remodeling of the PBVP (Fig. 4A-D). Corresponding serial sections were stained with hematoxylin and eosin (Fig. 4A, C) or co-stained with antibodies to endothelial cell PECAM-1 and α-SMC actin (Fig. 4B, D). The fibrous septal duct wall appeared to thicken and gain cellularity following As(III) exposure (Fig. 4C compared with 4A). Immunofluorescent analysis indicated that As(III) caused more pronounced PECAM-1–positive and PECAM/SMC-positive luminal structures in the septal wall (Fig. 4D versus 4B). Arsenic(III) increased the number of ductal vessels in the PBVP (Fig. 4E) and decreased hepatic artery luminal diameter by 3.5-fold (Fig. 4D compared to 4B and graph 4F).

As(III) Increases Caveolin-1 and Membrane Rac1 Protein Expression in SECs

SEC defenestration and capillarization should be associated with functional changes in cell signaling. Fenestrated endothelium have decreased expression of caveolin-1 and loss or fusion of caveolae.[36,37] To determine whether As(III) reversed suppression of SEC caveolin-1 expression, liver sections were co-immunostained for caveolin-1 and PECAM-1. The confocal images in Fig. 5A and graph in Fig. 5B con-firmed that caveolin-1 expression in normal sinusoids is low. Exposure to As(III) increased liver caveolin-1 expression by 5-fold to 6-fold over control and this increase was localized to PECAM-1 positive sinusoidal cells. This increase in caveolin-1 staining correlated with the increase in caveolae observed by TEM (Fig. 2). In angiogenesis, Rac1-GTPase regulates endothelial cell cytoskeletal fibers to stabilize the vessel phenotype with tight cell associations and spreading on a laminin-1 ECM.[34] Immuno-blotting for Rac1 in SEC plasma membranes isolated *in situ* demonstrated that membrane-bound GTPase was present in SECs from As(III)-exposed mice (Fig. 6) and not in SEC membranes from controls. The data in Fig. 6 also demonstrate that chronic As(III) exposure did not stimulate Rac1 membrane localization in other non-parenchymal cells or hepatocytes.

Discussion

Environmental As(III) exposures increase the incidence of liver diseases, such as noncirrhotic fibrosis and portal hypertension, in humans.[2] These As(III)-associated diseases present with liver vascular changes including increased vascular channels and arteriovenous shunts.[2] While angiogenesis and SEC maturation appear to play significant roles in disrupting sinusoidal

NIH-PA Author Manuscript

NIH-PA Author Manuscript

NIH-PA Author Manuscript

vessels,[18,22–25] the data presented here are the first to demonstrate that a human-relevant As (III) exposure induces capillarization and remodels the liver vasculature *in vivo*. These vascular phenotypic changes appear to be more sensitive biomarkers for As(III) exposure than As(III) levels quantified from liver tissue. These As(III)-induced changes in an endogenous vascular bed are consistent with previous reports that subchronic or chronic exposures to low to moderate levels of As(III) enhance pathological remodeling in surrogate neovascularization models and tumors.[7,9,28] Decreased SEC porosity and compensatory gain of caveolae represent potential mechanisms for As(III) to alter liver metabolism and contribute to systemic vascular diseases. Finally, these data are the first to demonstrate *in vivo* that As(III) affects endothelial cell signaling by increasing membrane localization Rac1.

The current data differ significantly from results from previous rodent studies of As(III) effects on the liver vasculature.[2,38–40] The major contrast is that vascular remodeling was observed following chronic exposure to a moderate As(III) exposure. One previous mouse study demonstrated that prolonged (9 month) exposure to high-dose As(III) (50–500 μg/mouse/day by gavage) resulted in liver lipid peroxidation and cytokine release.[38] These doses would be the equivalent of a human drinking 2–20 mg of As(III) perday for approximately 26 years before inflammatory toxicity occurred. This does not fit the demographic of As(III)-induced liver disease in humans, because significant increases in urinary porphyrins, a biomarker for liver injury, are more readily observed in exposed humans who are under 20 years of age.[4] *In vivo*, high doses of As(III) affect all cells in the liver and promote significant apoptosis in hepatocytes,[40] and doses of As(III) in excess of 5 μM are toxic to endothelial cells.[6,8,10,41] It is possible that high-level exposures elicit multiple mechanisms for toxicity that mask pathogenic mechanisms mediating liver diseases in response to environmentally relevant As (III) exposures. The current studies used ingestion of drinking water containing a dose of As (III) that is near the threshold for observing significant liver disease in humans (250 ppb = ~0.7–.9 μg/mouse/day for 5 weeks; human equivalent ~32 μg/day for 3.75 years) to investigate effects on the vasculature. Thus, the data reflect the effects of As(III) on cell phenotype rather than cell death.

Capillarization of hepatic sinusoids results in ultra-structural phenotypic conversion to defenestrated endothelial cells with tight intercellular junctions.[16,19,20] In multiple human and animal studies, capillarization preceded alcohol-induced liver disease, portal hypertension, cirrhosis, and chronic hepatitis.[15,18–20] Arsenic(III) induced SEC PECAM-1 expression and laminin-1 deposition in the basement membrane (Fig. 3) and correlated directly with decreased porosity and increased capillarization (Figs. 1 and 2). The data in Fig. 6 confirm that As(III) stimulated SEC Rac1 membrane mobilization and indicate that this localization was sustained in SECs during chronic As(III) exposure. Because Rac1 regulates endothelial cell spreading on laminin-1 matrices during angiogenic vessel maturation,[34] it is possible that sustained SEC Rac1 activation indicates chronic cell signaling changes that support capillarization in response to As(III) exposure.

Arsenic(III) may stimulate capillarization by disrupting the SEC signaling that maintains fenestrations and suppresses cell spreading. Tonic stimulation by VEGF promotes fenestrations and suppresses caveolae in cultured endothelial cells and in a number of vascular beds *in vivo*.[37,42] In SECs, this maintenance is mediated by stimulated nitric oxide (NO) synthesis.[15] Arsenic(III) inhibits agonist-stimulated NO synthesis in aortic endothelial cells,[43] and *in vivo* exposure to As(III) limits blood vessel vasoreactivity.[44] These inhibitory effects are mediated by As(III)-stimulated NADPH oxidase generation of super-oxide[43] that consumes NO[45] or by decreasing tetrahydrobiopterin levels required for NO synthase activity.[44] The data in Fig. 6 would be consistent with an As(III)-stimulated oxidative state in the SEC, because Rac1 is an essential component for As(III)-stimulated endothelial cell NADPH oxidase.[46–48] Disrupted VEGF signaling may explain the increase in SEC caveolin-1 expression (Fig. 5).

NIH-PA Author Manuscript

NIH-PA Author Manuscript

NIH-PA Author Manuscript

[37] However, caveolae (Fig. 2) and caveolin-1 (Fig. 5) may have increased to compensate for the reduced "passive" transendothelial transport because the SEC porosity is significantly diminished. Increased SEC caveolin-1 would further limit NO generation by sequestering and inhibiting endothelial NO synthase.[49]

In summary, these studies are the first to demonstrate that moderate environmental exposure to As(III) stimulates sinusoidal capillarization and vascular remodeling of the PBVP. These results are novel in revealing functional remodeling of an endogenous vascular bed in As(III)-exposed animals. The exposures were not long enough to observe portal fibrosis or changes in portal blood flow; however, the observed SEC changes were consistent with the pathogenesis of intrahepatic vascular disease and development of arteriovenous shunts observed in As(III)-induced human liver diseases.[2] Moreover, *in vivo* exposure of the liver vasculature is a suitable model for studying arsenic-induced effects that promote both pathogenic vascular cell responses and liver disease. Further studies using this model will be needed to identify the molecular switches through which As(III) stimulates phenotypic change in SECs without promoting hepatocyte injury. These studies will have great impact on the understanding of the mechanisms for human liver and vascular diseases associated with chronic environmental exposures to arsenic.

Acknowledgements

We thank Dr. Simon Watkins of the Center for Biologic Imaging for confocal and electron microscope time and Marc Rubin and Katie Clark for assistance in electron microscopy. We also thank Dr. Miroslav Styblo, University of North Carolina, for interpretation of tissue arsenic analyses and Dr. David J. Thomas, USEPA, for use of analytical instrumentation.

References

1. Navas-Acien A, Sharrett AR, Silbergeld EK, Schwartz BS, Nachman KE, Burke TA, et al. Arsenic exposure and cardiovascular disease: a systematic review of the epidemiologic evidence. Am J Epidemiol 2005;162:1037–1049. [PubMed: 16269585]
2. Mazumder DN. Effect of chronic intake of arsenic-contaminated water on liver. Toxicol Appl Pharmacol 2005;206:169–175. [PubMed: 15967205]
3. Guha Mazumder DN. Chronic arsenic toxicity: clinical features, epidemiology, and treatment: experience in West Bengal. J Environ Sci Health A 2003;38:141–163.
4. Ng JC, Wang JP, Zheng B, Zhai C, Maddalena R, Liu F, et al. Urinary porphyrins as biomarkers for arsenic exposure among susceptible populations in Guizhou province, China. Toxicol Appl Pharmacol 2005;206:176–184. [PubMed: 15967206]
5. Shigeno K, Naito K, Sahara N, Kobayashi M, Nakamura S, Fujisawa S, et al. Arsenic trioxide therapy in relapsed or refractory japanese patients with acute promyelocytic leukemia: updated outcomes of the phase II study and postremission therapies. Int J Hematol 2005;82:224–229. [PubMed: 16207595]
6. Kao YH, Yu CL, Chang LW, Yu HS. Low concentrations of arsenic induce vascular endothelial growth factor and nitric oxide release and stimulate angiogenesis in vitro. Chem Res Toxicol 2003;16:460–468. [PubMed: 12703962]
7. Soucy NV, Mayka D, Klei LR, Nemec AA, Bauer JA, Barchowsky A. Neovascularization and angiogenic gene expression following chronic arsenic exposure in mice. Cardiovasc Toxicol 2005;5:29–42. [PubMed: 15738583]
8. Barchowsky A, Dudek EJ, Treadwell MD, Wetterhahn KE. Arsenic induces oxidant stress and NF-kappaB activation in cultured aortic endothelial cells. Free Radic Biol Med 1996;21:783–790. [PubMed: 8902524]
9. Soucy NV, Ihnat MA, Kamat CD, Hess L, Post MJ, Klei LR, et al. Arsenic stimulates angiogenesis and tumorigenesis in vivo. Toxicol Sci 2003;76:271–279. [PubMed: 12970581]
10. Roboz GJ, Dias S, Lam G, Lane WJ, Soignet SL, Warrell RP Jr, et al. Arsenic trioxide induces dose- and time-dependent apoptosis of endothelium and may exert an antileukemic effect via inhibition of angiogenesis. Blood 2000;96:1525–1530. [PubMed: 10942401]

NIH-PA Author Manuscript

NIH-PA Author Manuscript

NIH-PA Author Manuscript

11. Lew YS, Brown SL, Griffin RJ, Song CW, Kim JH. Arsenic trioxide causes selective necrosis in solid murine tumors by vascular shutdown. Cancer Res 1999;59:6033–6037. [PubMed: 10626785]
12. Soucy NV, Klei LR, Mayka DD, Barchowsky A. Signaling pathways for arsenic-stimulated vascular endothelial growth factor-a expression in primary vascular smooth muscle cells. Chem Res Toxicol 2004;17:555–563. [PubMed: 15089098]
13. Braet F, Wisse E. Structural and functional aspects of liver sinusoidal endothelial cell fenestrae: a review. Comp Hepatol 2002;1:1–17. [PubMed: 12437787]
14. Couvelard A, Scoazec JY, Dauge MC, Bringuier AF, Potet F, Feldmann G. Structural and functional differentiation of sinusoidal endothelial cells during liver organogenesis in humans. Blood 1996;87:4568–4580. [PubMed: 8639825]
15. DeLeve LD, Wang X, Hu L, McCuskey MK, McCuskey RS. Rat liver sinusoidal endothelial cell phenotype is maintained by paracrine and autocrine regulation. Am J Physiol Gastrointest Liver Physiol 2004;287:G757–G763. [PubMed: 15191879]
16. Couvelard A, Scoazec JY, Feldmann G. Expression of cell-cell and cell-matrix adhesion proteins by sinusoidal endothelial cells in the normal and cirrhotic human liver. Am J Pathol 1993;143:738–752. [PubMed: 8362973]
17. Guyot C, Lepreux S, Combe C, Doudnikoff E, Bioulac-Sage P, Balabaud C, et al. Hepatic fibrosis and cirrhosis: The (myo)fibroblastic cell subpopulations involved. Int J Biochem Cell Biol 2006;38:135–151. [PubMed: 16257564]
18. Tsuneyama K, Ohba K, Zen Y, Sato Y, Niwa H, Minato H, et al. A comparative histological and morphometric study of vascular changes in idiopathic portal hypertension and alcoholic fibrosis/cirrhosis. Histopathology 2003;43:55–61. [PubMed: 12823713]
19. Dubuisson L, Boussarie L, Bedin CA, Balabaud C, Bioulac-Sage P. Transformation of sinusoids into capillaries in a rat model of selenium-induced nodular regenerative hyperplasia: an immunolight and immunoelectron microscopic study. Hepatology 1995;21:805–814. [PubMed: 7875679]
20. Xu B, Broome U, Uzunel M, Nava S, Ge X, Kumagai-Braesch M, et al. Capillarization of hepatic sinusoid by liver endothelial cell-reactive auto-antibodies in patients with cirrhosis and chronic hepatitis. Am J Pathol 2003;163:1275–1289. [PubMed: 14507637]
21. Li J, Niu JZ, Wang JF, Li Y, Tao XH. Pathological mechanisms of alcohol-induced hepatic portal hypertension in early stage fibrosis rat model. World J Gastroenterol 2005;11:6483–6488. [PubMed: 16425420]
22. Ward NL, Haninec AL, Van Slyke P, Sled JG, Sturk C, Henkelman RM, et al. Angiopoietin-1 causes reversible degradation of the portal microcirculation in mice: implications for treatment of liver disease. Am J Pathol 2004;165:889–899. [PubMed: 15331413]
23. Semela D, Dufour JF. Angiogenesis and hepatocellular carcinoma. J Hepatol 2004;41:864–880. [PubMed: 15519663]
24. Moreau R. VEGF-induced angiogenesis drives collateral circulation in portal hypertension. J Hepatol 2005;43:6–8. [PubMed: 15893843]
25. Fernandez M, Mejias M, Angermayr B, Garcia-Pagan JC, Rodes J, Bosch J. Inhibition of VEGF receptor-2 decreases the development of hyperdynamic splanchnic circulation and portal-systemic collateral vessels in portal hypertensive rats. J Hepatol 2005;43:98–103. [PubMed: 15893841]
26. Cogger VC, Muller M, Fraser R, McLean AJ, Khan J, Le Couteur DG. The effects of oxidative stress on the liver sieve. J Hepatol 2004;41:370–376. [PubMed: 15336438]
27. Hilmer SN, Cogger VC, Fraser R, McLean AJ, Sullivan D, Le Couteur DG. Age-related changes in the hepatic sinusoidal endothelium impede lipoprotein transfer in the rat. Hepatology 2005;42:1349–1354. [PubMed: 16317689]
28. Kamat CD, Green DE, Curilla S, Warnke L, Hamilton JW, Sturup S, et al. Role of HIF signaling on tumorigenesis in response to chronic low-dose arsenic administration. Toxicol Sci 2005;86:248–257. [PubMed: 15888669]
29. Hughes MF, Devesa V, Adair BM, Styblo M, Kenyon EM, Thomas DJ. Tissue dosimetry, metabolism and excretion of pentavalent and trivalent monomethylated arsenic in mice after oral administration. Toxicol Appl Pharmacol 2005;208:186–197. [PubMed: 16183392]

NIH-PA Author Manuscript

NIH-PA Author Manuscript

NIH-PA Author Manuscript

30. Lagoa CE, Vodovotz Y, Stolz DB, Lhuillier F, McCloskey C, Gallo D, et al. The role of hepatic type 1 plasminogen activator inhibitor (PAI-1) during murine hemorrhagic shock. Hepatology 2005;42:390–399. [PubMed: 16025510]
31. Stolz DB, Ross MA, Salem HM, Mars WM, Michalopoulos GK, Enomoto K. Cationic colloidal silica membrane perturbation as a means of examining changes at the sinusoidal surface during liver regeneration. Am J Pathol 1999;155:1487–1498. [PubMed: 10550305]
32. Devesa V, Paul DS, Thomas DJ, Styblo M. Tissue distribution of arsenic species in mice chronically exposed to arsenite or methylarsonous acid [Abstract 413]. Toxicologist 2006;90(Suppl):85.
33. Wack KE, Ross MA, Zegarra V, Sysko LR, Watkins SC, Stolz DB. Sinusoidal ultrastructure evaluated during the revascularization of regenerating rat liver. Hepatology 2001;33:363–378. [PubMed: 11172338]
34. Davis GE, Senger DR. Endothelial extracellular matrix: biosynthesis, remodeling, and functions during vascular morphogenesis and neovessel stabilization. Circ Res 2005;97:1093–1107. [PubMed: 16306453]
35. Neubauer K, Wilfling T, Ritzel A, Ramadori G. Platelet-endothelial cell adhesion molecule-1 gene expression in liver sinusoidal endothelial cells during liver injury and repair. J Hepatol 2000;32:921–932. [PubMed: 10898312]
36. Braet F. How molecular microscopy revealed new insights into the dynamics of hepatic endothelial fenestrae in the past decade. Liver Int 2004;24:532–539. [PubMed: 15566501]
37. Esser S, Wolburg K, Wolburg H, Breier G, Kurzchalia T, Risau W. Vascular endothelial growth factor induces endothelial fenestrations in vitro. J Cell Biol 1998;140:947–959. [PubMed: 9472045]
38. Das S, Santra A, Lahiri S, Guha Mazumder DN. Implications of oxidative stress and hepatic cytokine (TNF-alpha and IL-6) response in the pathogenesis of hepatic collagenesis in chronic arsenic toxicity. Toxicol Appl Pharmacol 2005;204:18–26. [PubMed: 15781290]
39. Flora SJ, Pant SC, Malhotra PR, Kannan GM. Biochemical and histopathological changes in arsenic-intoxicated rats coexposed to ethanol. Alcohol 1997;14:563–568. [PubMed: 9401671]
40. Bashir S, Sharma Y, Irshad M, Nag TC, Tiwari M, Kabra M, et al. Arsenic induced apoptosis in rat liver following repeated 60 days exposure. Toxicology 2006;217:63–70. [PubMed: 16288947]
41. Barchowsky A, Roussel RR, Klei LR, James PE, Ganju N, Smith KR, et al. Low levels of arsenic trioxide stimulate proliferative signals in primary vascular cells without activating stress effector pathways. Toxicol Appl Pharmacol 1999;159:65–75. [PubMed: 10448126]
42. Maharaj AS, Saint-Geniez M, Maldonado AE, D'Amore PA. Vascular endothelial growth factor localization in the adult. Am J Pathol 2006;168:639–648. [PubMed: 16436677]
43. Barchowsky A, Klei LR, Dudek EJ, Swartz HM, James PE. Stimulation of reactive oxygen, but not reactive nitrogen species, in vascular endothelial cells exposed to low levels of arsenite. Free Radic Biol Med 1999;27:1405–1412. [PubMed: 10641735]
44. Pi J, Horiguchi S, Sun Y, Nikaido M, Shimojo N, Hayashi T, et al. A potential mechanism for the impairment of nitric oxide formation caused by prolonged oral exposure to arsenate in rabbits. Free Radic Biol Med 2003;35:102–113. [PubMed: 12826260]
45. Bunderson M, Brooks DM, Walker DL, Rosenfeld ME, Coffin JD, Beall HD. Arsenic exposure exacerbates atherosclerotic plaque formation and increases nitrotyrosine and leukotriene biosynthesis. Toxicol Appl Pharmacol 2004;201:32–39. [PubMed: 15519606]
46. Smith KR, Klei LR, Barchowsky A. Arsenite stimulates plasma membrane NADPH oxidase in vascular endothelial cells. Am J Physiol 2001;280:L442–L449.
47. Brown JH, Del Re DP, Sussman MA. The Rac and Rho hall of fame: a decade of hypertrophic signaling hits. Circ Res 2006;98:730–742. [PubMed: 16574914]
48. Ushio-Fukai M, Alexander RW. Reactive oxygen species as mediators of angiogenesis signaling: role of NAD(P)H oxidase. Mol Cell Biochem 2004;264:85–97. [PubMed: 15544038]
49. Shah V, Cao S, Hendrickson H, Yao J, Katusic ZS. Regulation of hepatic eNOS by caveolin and calmodulin after bile duct ligation in rats. Am J Physiol Gastrointest Liver Physiol 2001;280:G1209–G1216. [PubMed: 11352814]

NIH-PA Author Manuscript

NIH-PA Author Manuscript

NIH-PA Author Manuscript

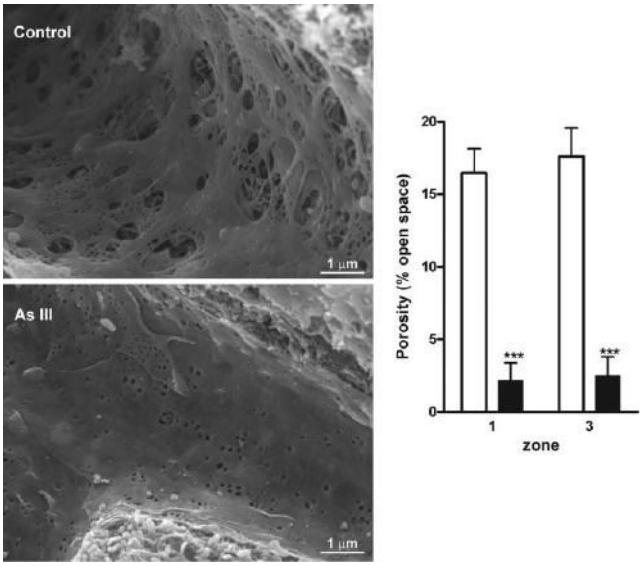

Fig. 1.

Arsenic-stimulated capillarization of the liver sinusoidal endothelium. SEM images of sinusoidal vessels were obtained from thick sections of livers excised from control mice or mice exposed to 250 ppb As(III) for 5 weeks. In the graph, data are presented as mean ± SD porosity (open bars = control, closed bars = As(III)-exposed, $n = 3$), as determined in experimental procedures. Two-way ANOVA and Bonferroni's post-test demonstrated no significant differences between zones, a highly significant effect of arsenic exposure relative to control (***$P < 0.001$).

NIH-PA Author Manuscript

NIH-PA Author Manuscript

NIH-PA Author Manuscript

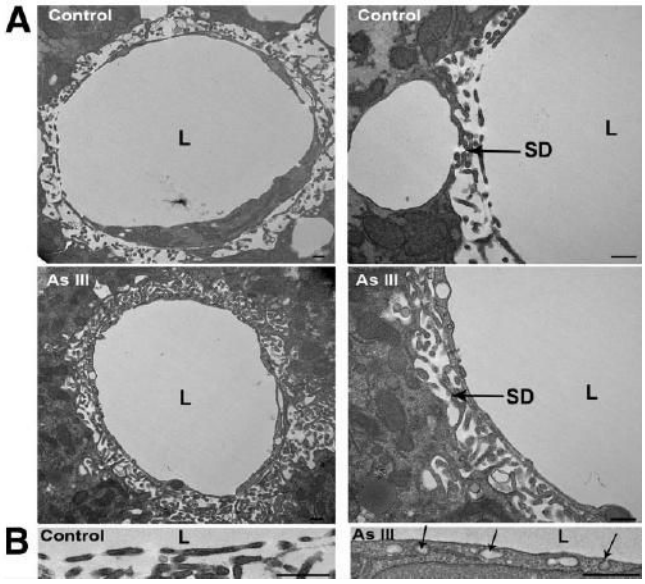

Fig. 2.

Arsenic-stimulated capillarization, basement membrane formation, and increased hepatocyte microvilli. (A) TEM images of sinusoidal vessels were captured from ultrathin sections of livers. Representative images are presented with portions magnified (B) to illustrate changes in the space of Disse and to show increased caveolae (arrows) in As(III)-exposed mice. (Bars = 500 nm) Abbreviations: SD, space of Disse; L, sinusoid lumen.

NIH-PA Author Manuscript

NIH-PA Author Manuscript

NIH-PA Author Manuscript

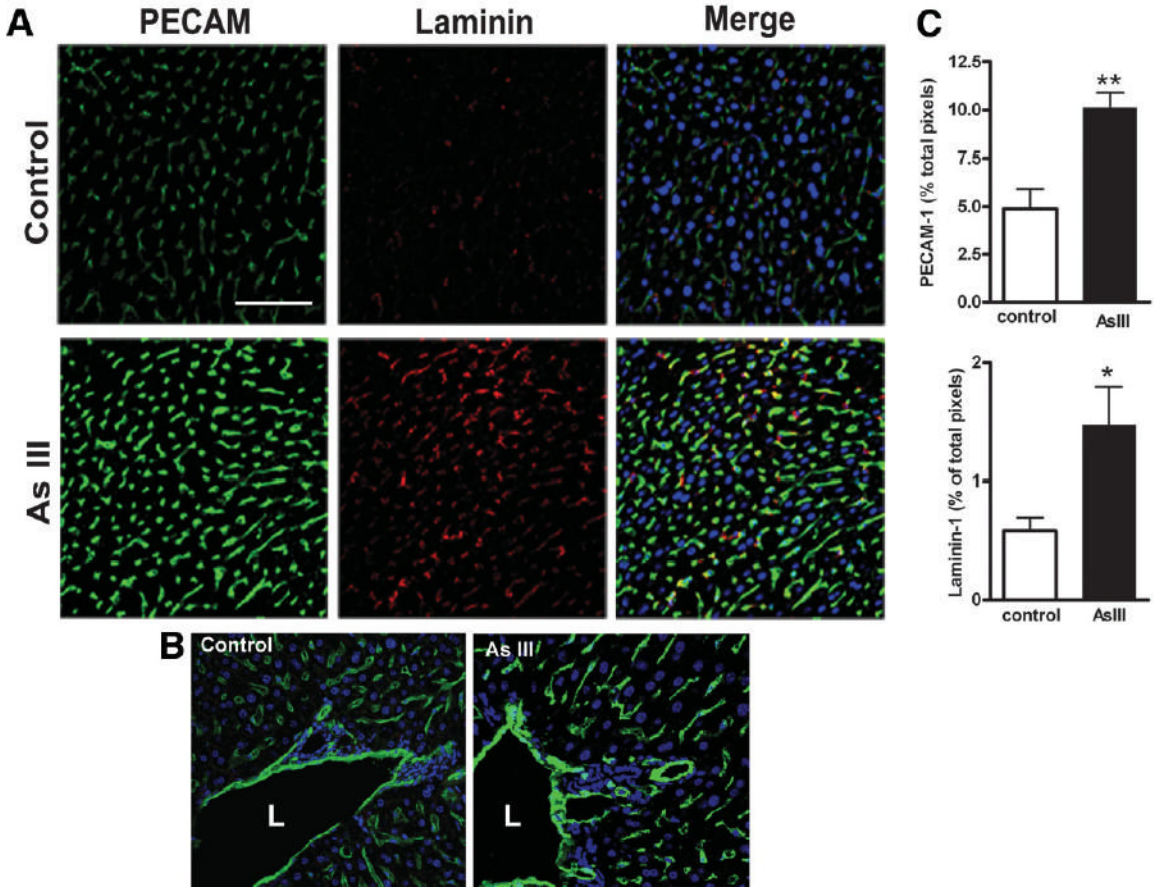

Fig. 3.

Arsenic(III) induced expression of sinusoidal PECAM-1 and laminin protein. (A) Cryosections were immunostained for PECAM-1 (green) or laminin-1 (red). Merged images show DRAQ 5 stained nuclei (blue) (bar = 50 μm). (B) Images of portal vein and periportal PECAM-1 (green) and nuclear staining demonstrate PECAM changes in sinusoids, but not in the portal vein endothelium (L = lumen). (C) Quantitative morphometric analysis of midlobular PECAM-1 and laminin-1 protein staining is presented as the mean ± SD percentage of total positive-staining pixels for the respective protein per 400× microscopic field (**$P < 0.01$ and *$P < 0.05$, n = 5 mice).

NIH-PA Author Manuscript

NIH-PA Author Manuscript

NIH-PA Author Manuscript

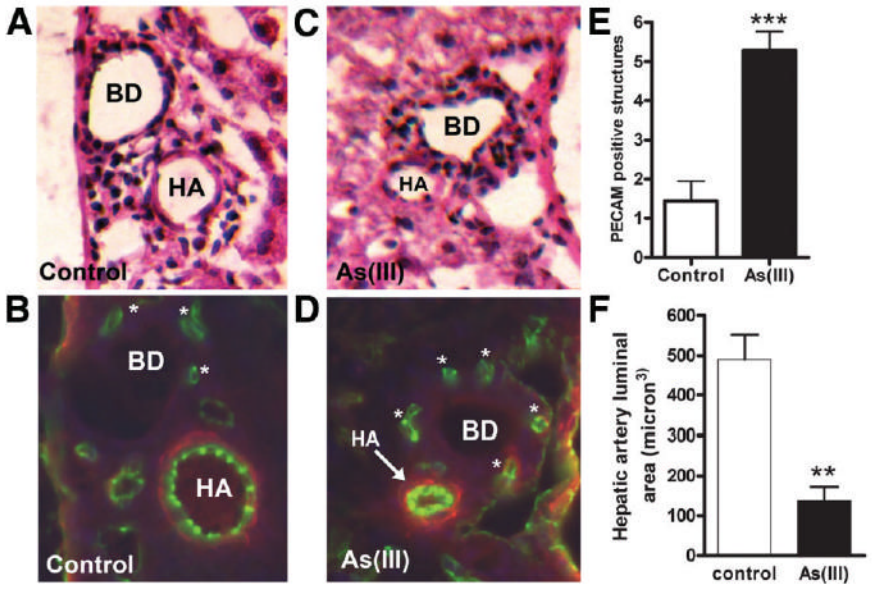

Fig. 4.

As(III) stimulates vascularization of the PBVP and hepatic artery contraction. Serial sections were prepared from livers from control or As(III)-exposed mice. Sections were stained with either hematoxylin & eosin [(A) and (C)] or immunostained for PECAM-1 (green) and α-SMC actin (red) [(B) and (D)]. Final image magnification was 400× (BD = biliary ducts, HA = hepatic arteries). (E) The mean ± SD of PECAM-positive structures [* in images (B) and (D)] surrounding at least 2 biliary ducts per section from 5 mice is presented (***$P < 0.001$). (F) The luminal areas of hepatic arterioles were calculated. The data are the mean ± SD of the average luminal areas of at least 2 hepatic arterioles per section from 5 mice in each group. (**$P < 0.01$).

NIH-PA Author Manuscript
NIH-PA Author Manuscript
NIH-PA Author Manuscript

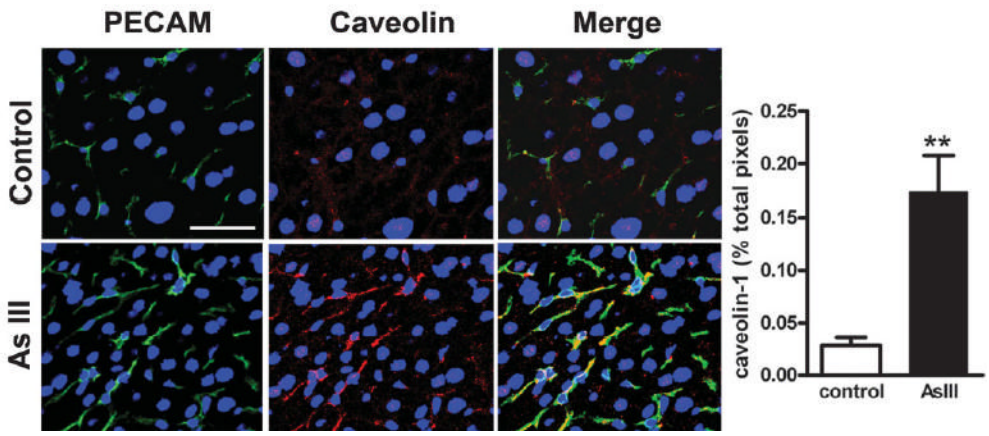

Fig. 5.

Co-localization of As(III)-stimulated caveolin-1 and PECAM-1 protein expression. Sections of livers were immunostained for PECAM-1 (green) or caveolin-1 (red). Nuclei were stained with DRAQ 5 (blue). The white bar = 25 μm. The graph presents mean ± SD percentage of caveolin-1 positive pixels per 400× microscopic field (**$P < 0.01$; $n = 5$).

NIH-PA Author Manuscript
NIH-PA Author Manuscript
NIH-PA Author Manuscript

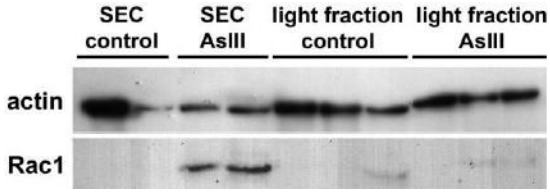

Fig. 6.

Chronic As(III)-stimulated mobilization of Rac1 to SEC luminal membranes. Luminal SEC membranes of control and As(III) exposed mice were separated from total liver cell membranes (light fraction), as described in "Materials and Methods". Rac1 and actin (loading control) abundance was measured by Western blotting. Each lane presents protein abundance in liver and SEC membrane fractions from individual mice.

NIH-PA Author Manuscript
NIH-PA Author Manuscript
NIH-PA Author Manuscript

Table 1

Antibodies Used in Immunofluorescence and Western Analysis

Antigen	Protocol	1° Antibody Source (Dilution)	2° Antibody Source/Fluorophor (Dilution)
PECAM (CD31)	IF	Monoclonal rat anti-mouse CD31 (clone-MEC13.3) BD Biosciences, San Jose, CA (1:100)	Goat anti-rat Alexa 488, Invitrogen, Carlsbad, CA (1:500)
Laminin-1	IF	Polyclonal rabbit anti-laminin Sigma, St. Louis, MO (1:750)	Goat anti-rabbit Alexa 594, Invitrogen (1:500)
Caveolin-1	IF	Polyclonal rabbit anti-caveolin-1, Cell Signaling Technologies, Danvers, MA (1:300)	Goat anti-rabbit Alexa 594, Invitrogen (1:500)
αSMA	IF	Monoclonal anti-alpha smooth muscle actin (clone 1A4), Sigma (1:500)	Goat anti-mouse Alexa 594, Invitrogen (1:500)
Actin	WB	Monoclonal mouse anti-actin (clone C4) Chemicon, Temecula, CA (1:1000)	Sheep anti-mouse HRP, GE Healthcare, Piscataway, NJ (1:5000)
Rac1	WB	Monoclonal mouse anti-rac1 (clone-102), BD Biosciences (1:1000)	Sheep anti-mouse HRP, GE Healthcare (1:5000)
Nucleus	IF	Not applicable	DRAQ5, Biostatus, Leicestershire, UK (1:2000)

Abbreviations: IF, immunofluorescence; WB, western blot.